Am J Nucl Med Mol Imaging 2025;15(3):87-96
www.ajnmmi.us /ISSN:2160-8407/ajnmmi0163903

Original Article

[^{89}Zr]Zr-DFO-Trodelvy immunoPET for noninvasive Trop2 imaging in bladder cancer

Wenpeng Huang[1,2*], Xinyao Sun[1*], Yutong Liang[3], Jason C Mixdorf[2], Qi Yang[1], Jonathan W Engle[2], Xiaoyan Xiao[4], Liming Li[4], Lei Kang[1], Weibo Cai[2]

[1]Department of Nuclear Medicine, Peking University First Hospital, Beijing 100034, China; [2]Departments of Radiology and Medical Physics, University of Wisconsin - Madison, Madison, WI 53705, USA; [3]Michigan State University College of Osteopathic Medicine, East Lansing, MI 48824, USA; [4]Department of Radiology, The First Affiliated Hospital of Zhengzhou University, Zhengzhou 450052, Henan, China. [*]Equal contributors.

Received February 13, 2025; Accepted June 15, 2025; Epub June 25, 2025; Published June 30, 2025

Abstract: Purpose: The Trop2-targeting antibody-drug conjugate (ADC), sacituzumab govitecan (Trodelvy™), demonstrates significant therapeutic efficacy in targeting Trop2-expressing tumors. In this study, we utilized immunoPET imaging to assess Trop2 expression in bladder cancer models using [^{89}Zr]Zr-DFO-Trodelvy. Materials and methods: Trop2 expression levels in bladder cancer cell lines were measured using flow cytometry and immunofluorescence staining. Radiolabeling of DFO-Trodelvy with ^{89}Zr was carried out in Na_2CO_3 buffer at pH 7 (37°C, 1.5 h). ImmunoPET imaging with [^{89}Zr]Zr-DFO-Trodelvy was performed at multiple time points to evaluate *in vivo* targeting. Additionally, tumor tissues from tumor-bearing mice were analyzed by immunofluorescence. Results: The radiochemical yield of [^{89}Zr]Zr-DFO-Trodelvy was >90%, with radiochemical purity exceeding 99%. Trop2 expression was high in HT1376 cells and low in T24 cells. ImmunoPET imaging demonstrated effective visualization of tumors in HT1376 models as early as 6 h post-injection, with tumor uptake reaching peak at 48 h (16.33 ± 0.90 %ID/g), followed by a gradual decline. In contrast, T24 tumors showed significantly lower uptake (6.20 ± 0.99 %ID/g, P = 0.0005). Co-injection with 2 mg of unlabeled Trodelvy significantly reduced tumor uptake in HT1376 models (4.50 ± 0.51 %ID/g, P = 0.0004), confirming target specificity. At 48 h, a high tumor-to-background ratio was observed, indicating selective accumulation in tumor tissue. Conclusions: [^{89}Zr]Zr-DFO-Trodelvy enables precise immunoPET imaging of bladder cancer models with high Trop2 expression, demonstrating specific and sustained tumor accumulation. These findings highlight the potential of this imaging approach for the noninvasive assessment of Trop2 expression.

Keywords: Zr-89, Trop2, immunoPET, antibody-drug conjugate, radioactive tracer, bladder cancer

Introduction

Bladder cancer currently remains as one of the leading cancers and cancer-related mortality worldwide. It significantly impacts quality of life for patients while increasing morbidity, mortality, and healthcare costs [1]. While surgery remains the primary treatment for bladder cancer, it is frequently supplemented with immunotherapy and targeted therapies [2, 3]. However, patients receiving anti-PD-L1 checkpoint inhibitors following platinum-based treatments, or those deemed ineligible for cisplatin, often face poor prognoses with limited therapeutic options, highlighting the urgent need for the development of more effective treatment strategies [4].

The development of novel, noninvasive biomarkers and imaging modalities that can enhance early detection and disease monitoring is crucial to improving survival outcomes through timely intervention [5, 6]. In recent years, significant progress has been made in understanding the molecular mechanisms underlying bladder cancer development and progression. Trophoblast cell surface antigen 2 (Trop2) is a cell surface glycoprotein with stem cell-like properties that contributes to organogenesis and embryonic development, while also playing a pivotal role in tumor progression by promoting tumor growth, proliferation, and migration. This process is mediated through multiple molecular mechanisms, including the regulation of calcium signaling pathways, modulation of cyclin expression, and facilitation of epithelial-mesenchymal transition (EMT), which reduces cell adhesion and enhances the invasive and migratory capability of tumor cells [7-10]. Importantly, Trop2 is either absent or minimally expressed in normal tissues, making it an attractive therapeutic target for cancer therapy due to its minimal off-target toxicity [9]. Elevated Trop2 expression has been particularly noted in bladder cancer [11, 12].

In 2021, the Trop2-targeting antibody-drug conjugate (ADC) sacituzumab govitecan (Trodelvy™) was developed and demonstrated significant efficacy in patients with metastatic triple-negative breast cancer [13, 14]. The concept for treatment in both breast and bladder cancer is the same, with high expression of Trop2 driving tumor progression and emphasizing the potential of this ADC to selectively target and accumulate within tumors [15]. Consequently, immunoPET represents an innovative advancement in molecular imaging, combining an antibody or related molecule with a positron- or gamma-emitting radionuclide to enable the *in vivo* visualization of spe-

https://doi.org/10.62347/KKEE6954

cific antigens [16, 17]. Notably, the physical half-life of ^{89}Zr (78.4 h) aligns well with the extended biological half-life of antibodies (2-3 weeks), enabling high-resolution quantitative PET imaging [18].

In this study, we leveraged the enhanced targeting specificity of ADCs to perform immunoPET imaging of Trop2 expression in bladder cancer models using [^{89}Zr]Zr-DFO-Trodelvy.

Materials and methods

Differential expression and prognostic significance of Trop2 in GEPIA

The Gene Expression Profiling Interactive Analysis (GEPIA) is a online platform for analyzing RNA sequencing expression data derived from the Genotype-Tissue Expression (GTEx) and The Cancer Genome Atlas (TCGA) projects. Survival analyses, including overall survival (OS) and disease-free survival (DFS), were performed across 33 distinct cancer types using GEPIA, employing the log-rank and Mantel-Cox tests. Additionally, correlation analyses were conducted across multiple TCGA expression datasets. GEPIA's "auto choose best cut-off" function determined the optimal cut-off values for survival curves by evaluating all possible thresholds between the lower and upper quartiles, selecting the most statistically significant threshold for mRNA expression levels. The results of this analysis provided key insights into Trop2's differential expression and its prognostic relevance within the GEPIA framework [19].

Conjugation and radiolabeling

Conjugation of *p*-SCN-Bn-DFO (Macrocyclics, Plano, USA) was performed at pH 9.0 for 2 h, with a DFO-to-Trodelvy molar ratio of 15:1. The resulting DFO-Trodelvy conjugates were purified using PD-10 columns, with PBS as the mobile phase, and the concentration was determined using a NanoDrop spectrophotometer (Thermo Scientific). ^{89}Zr was produced by a PET trace cyclotron via the ^{89}Y(p,n)^{89}Zr nuclear reaction. For radiolabeling, approximately 74 MBq (~2 mCi) of ^{89}Zr was added to 0.5 mM HEPES buffer (pH 7.0) and incubated with DFO-Trodelvy (~300 μg) at 37°C for 1.5 h. The [^{89}Zr]Zr-DFO-Trodelvy product was purified using a PD-10 column with PBS, and radioactive fractions containing the ^{89}Zr-labeled conjugate were collected and filtered through a 0.2 μm syringe filter for *in vivo* applications. Labeling efficiency and radiochemical purity were assessed using radio thin-layer chromatography (Radio-TLC) [20].

Cell culture

Human bladder cancer cells lines HT1376 and T24, were obtained from the American Type Culture Collection (ATCC, Manassas, VA, USA). HT1376 cells were cultured in RPMI 1640 medium (Invitrogen, Carlsbad, CA) supplemented with 10% fetal bovine serum (FBS) and maintained at 37°C in a 5% CO_2 incubator. T24 cells were cultured in Dulbecco's Modified Eagle Medium (DMEM; Gibco, USA). Both cell lines were utilized for *in vitro* or *in vivo* experiments once they reached 70%-80% confluence.

Animal model

All animal experiments adhered to protocols approved by the University of Wisconsin Institutional Animal Care and Use Committee (IACUC). For tumor model establishment, four to five-week-old female Athymic Nude-Foxn1nu mice were procured from Envigo (Indianapolis, IN). Tumors were induced by subcutaneous injection of 4-5 × 10^6 cells, suspended in a 70 μL mixture of PBS and Matrigel (1:1, Corning, USA), into the mice's front flank. Tumor growth was monitored every other day, with mice selected for *in vivo* experiments once tumor diameters reached 10-15 mm.

Flow cytometry

All cells were washed twice with cold PBS and adjusted to a final concentration of 10^5 cells/mL before analysis using the Lightning cytometer (ThermoFisher Attune). Immunostaining was performed with Trodelvy and DFO-Trodelvy at a final concentration of 40 μg/mL for 1 h on ice, in the dark. This was then followed by incubation with AF488-labeled anti-human secondary antibodies (Alexa Fluor 488) at room temperature (RT) for 0.5 h. Data acquisition and analysis were conducted using FlowJo software.

Cellular immunofluorescent staining

For the immunofluorescent staining assay, cells were seeded in 35 mm plates at a density of 2 × 10^5 cells and incubated overnight. Cells were then fixed with 4% paraformaldehyde at 4°C, followed by permeabilization with Triton X-100 at RT for 15 minutes. Next, the cells were incubated with Trodelvy (10 μg/mL), washed three times with cold PBS, and subsequently incubated with AF488-labeled rabbit anti-mouse secondary antibodies (Alexa Fluor 488) at RT for 30 minutes. After another three washes with cold PBS, the cells were stained with DAPI-containing mounting medium. Imaging was performed using an A1R confocal laser scanning microscope (Nikon, Inc., Melville, NY).

Cell uptake experiment

Cells were seeded in 24-well plates at a density of 2.0 × 10^5 cells/well (n = 3). Each well was then replaced with 1 mL of serum-free medium containing [^{89}Zr]Zr-DFO-Trodelvy (37 kBq) and incubated at 37°C for various time points (1, 2, and 4 h). Following incubation, 1 mL of 1 M NaOH was added for cell lysis, and lysates were collected. The radioactivity in both the supernatants and lysates was measured using an automatic gamma counter (PerkinElmer,

Wizard2). For blocking studies, cells were pre-incubated with an excess of unlabeled Trodelvy for 2 h prior to the experiments.

Cell binding assay

HT1376 and T24 cells were seeded into a 96-well filter plate at a density of 1.0×10^5 cells per well. A series of [^{89}Zr]Zr-DFO-Trodelvy solutions were prepared, and cells were incubated with these solutions for 4 h at 37°C, with final concentrations ranging from 0.01 to 300 nM (n = 3). To assess nonspecific binding, unlabeled Trodelvy (1 μM) was added in parallel. Following incubation, the cells were washed and analyzed using a gamma counter. The surface expression of Trop2, apparent dissociation constant (K_D), and maximum binding capacity (B_{max}) were calculated based on total and nonspecific binding data using GraphPad Prism (version 8.0) software.

ImmunoPET imaging

PET studies were carried out using an Inveon microPET scanner for rodents (Siemens Medical Solutions USA, Inc.). Tumor-bearing mice were administered 7.4-11.1 MBq of [^{89}Zr]Zr-DFO-Trodelvy via intravenous injection, with imaging performed at 6, 12, 24, 48, 72, 96, and 120 h post-injection (p.i.). Mice were anesthetized with 2% isoflurane and scanned in prone position. Images were calibrated to display signals ranging from 0 to 15% of the injected dose (ID) per volume, expressed as %ID/g. Quantitative analysis was performed by delineating regions of interest (ROI) in the heart, liver, kidneys, muscles, spleen and tumors, followed by calculating tumor-to-heart and tumor-to-muscle ratios.

Ex vivo biodistribution

Following the final imaging time point, mice were euthanized using carbon dioxide asphyxiation. Major organs and tissues, including the tumor, heart, liver, spleen, lungs, kidneys, stomach, intestines, muscles, bones, brain, and blood, were collected and weighed. Radioactivity in each sample was measured using an automated gamma counter, with biodistribution calculated as %ID/g.

Radiation dosimetry prediction

Female BALB/c mice (4 weeks old) were assigned to five groups (n = 3) and administered 0.74 MBq of [^{89}Zr]Zr-DFO-Trodelvy (100 μL) via tail vein injection. The mice were euthanized at 4, 24, 48, 72, and 96 h p.i. Extrapolated radiation doses for adult females were calculated based on decay-corrected ^{89}Zr biodistribution data. Dosimetry analysis was conducted using the OLINDA/EXM dose-spherical model within the OLINDA/EXM software [21].

Histological analysis

Histological evaluations included immunohistochemistry (IHC) and immunofluorescence staining. Trop2 expression was analyzed using IHC on human tissue sections, provided by The First Affiliated Hospital of Zhengzhou University. Immunofluorescence staining was performed on tumor tissues following standardized protocols to assess Trop2 expression [22, 23]. Primary antibodies included an anti-human Trop2 antibody (1:200, Bio-Legend) and an anti-human CD31 antibody (1:200, Servicebio). Secondary antibodies consisted of AF488-labeled goat anti-rabbit IgG (1:200, Servicebio) and Cy3-labeled goat anti-mouse IgG (1:200, Servicebio). Morphological features and staining patterns were examined and documented using a Nikon optical microscope or an Olympus confocal microscope.

Statistical analysis

Quantitative data were presented as mean ± standard deviation. Statistical evaluations were performed using the Student's *t*-test or one- or two-way ANOVA, with GraphPad Prism version 8.0. A *P*-value less than 0.05 was considered statistically significant.

Results

Differential expression and prognostic correlation of Trop2 in databases, and IHC staining of Trop2 in normal human tissues

TCGA and GTEx data from GEPIA were analyzed to assess the differential expression of Trop2 across various tumor and normal tissue types. As shown in **Figure 1A**, Trop2 expression was significantly elevated in certain tumor samples compared to normal tissues. **Figure 1B** illustrates the correlation between Trop2 expression and DFS in patients with colon adenocarcinoma (COAD), esophageal carcinoma (ESCA), pancreatic adenocarcinoma (PAAD), rectum adenocarcinoma (READ). To further evaluate Trop2 expression, immunohistochemical staining was conducted on eight normal human tissues - heart, lung, stomach, kidney, intestine, liver, spleen, and pancreas (**Figure 1C**).

Radiosynthesis of [^{89}Zr]Zr-DFO-Trodelvy

The labeling yield prior to purification was >90%. After purification using PD-10 columns, the radiochemical purity (RCP) of the tracers exceeded 99%, with no detectable free ^{89}Zr in the target fractions of [^{89}Zr]Zr-DFO-Trodelvy.

Flow cytometry and cellular immunofluorescent staining

Trop2 was highly expressed in HT1376 cells, as evidenced by Trodelvy's selective binding, and was marked by a pronounced shift in the fluorescent signal peak. In contrast, Trop2 expression was minimal in T24 cells. Importantly, the conjugation of Trodelvy with DFO did not compromise its binding affinity (**Figure 2A**). Immunofluorescence staining revealed intense Trop2 signals localized to the cell membrane in HT1376 cells, whereas no detectable sig-

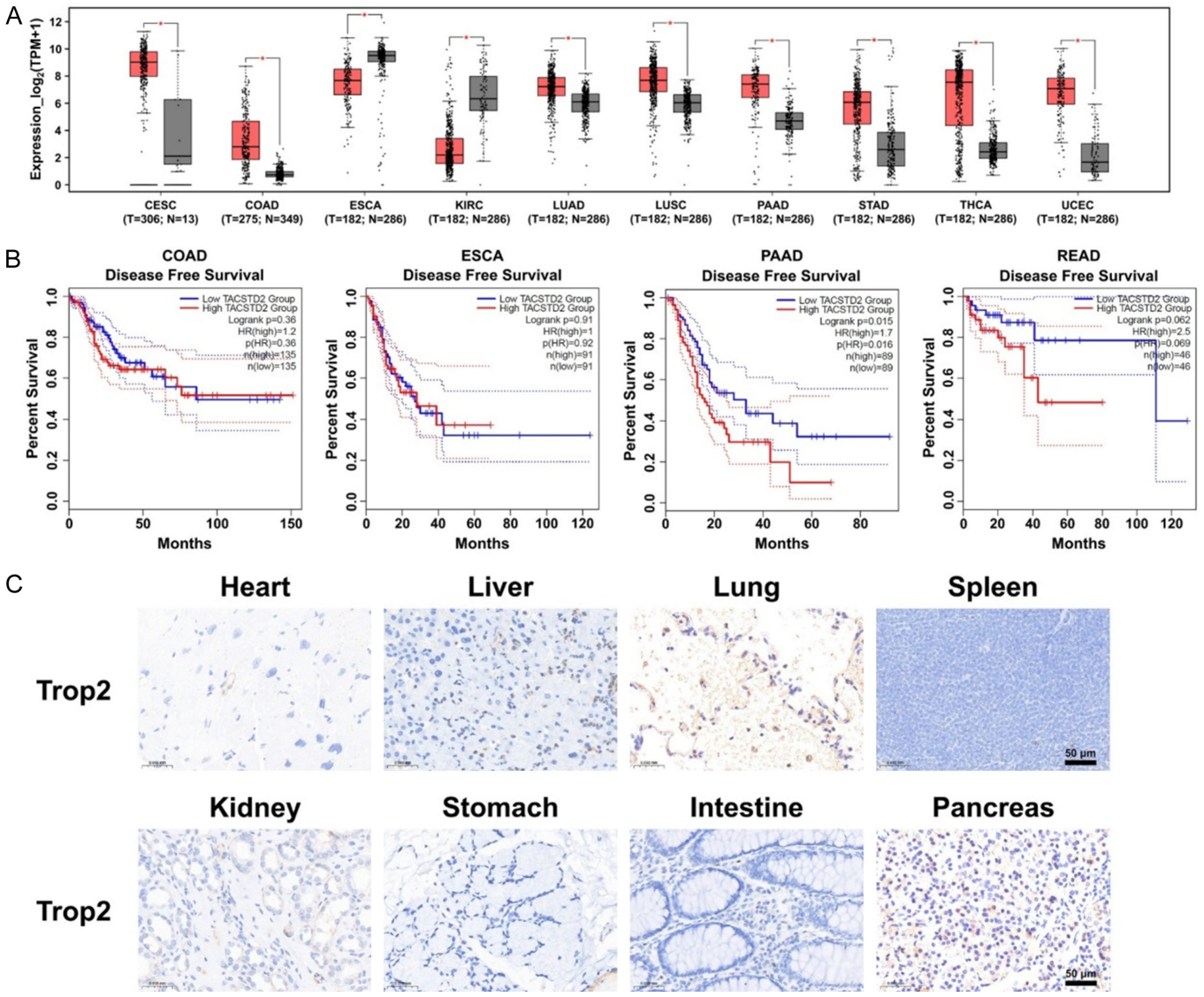

Figure 1. Differential expression and prognostic correlation of Trop2 in databases, and immunohistochemistry (IHC) staining of Trop2 in normal human tissues. A. Correlation analysis of Trop2 expression across solid tumors using TCGA and GTEx data. Box plots depict differential mRNA expression of Trop2 in tumor tissues (red) from TCGA compared to normal tissues (gray) from GTEx, with $*P < 0.01$ indicating statistical significance. B. Prognostic comparison of disease-free survival between high and low Trop2 expression in COAD, ESCA, PAAD, READ. Abbreviations: CESC: Cervical squamous cell carcinoma and endocervical adenocarcinoma; COAD: Colon adenocarcinoma; ESCA: Esophageal carcinoma; KIRC: Kidney renal clear cell carcinoma; LUAD: Lung adenocarcinoma; LUSC: Lung squamous cell carcinoma; PAAD: Pancreatic adenocarcinoma; STAD: Stomach adenocarcinoma; THCA: Thyroid carcinoma; UCEC: Uterine corpus endometrial carcinoma. C. IHC images illustrating Trop2 expression in normal human tissues, including heart, lung, stomach, kidney, intestine, liver, spleen, and pancreas. Scale bars: 50 μm.

nals were observed in T24 cells (**Figure 2B**). Based on this, HT1376 cells were identified as Trop2-overexpression models, while T24 cells served as negative controls.

Cell uptake assay and cell binding assay experiment

The uptake of HT1376 cells (n = 3) was 7.06 ± 1.32 %AD/2×10^5 at 1 h, 8.72 ± 1.38 %AD/2×10^5 at 2 h, and 7.45 ± 0.86 %AD/2×10^5 at 4 h, exhibiting a statistically significant increase compared to the T24 group (0.96 ± 0.14 %AD/2×10^5 at 1 h, 0.52 ± 0.04 %AD/2×10^5 at 2 h, and 0.27 ± 0.05 %AD/2×10^5 at 4 h). The specificity of uptake was confirmed by the addition of cold, unlabeled Trodelvy, which significantly reduced uptake levels to 0.81 ± 0.45 %AD/2×10^5 at 1 h (P = 0.0139), 0.27 ± 0.08 %AD/2×10^5 at 2 h (P = 0.0128), and 0.27 ± 0.05 %AD/2×10^5 at 4 h (P = 0.0070) (**Figure 3A**). The K_D of [^{89}Zr]Zr-DFO-Trodelvy for HT1376 cells (n = 3) was determined to be 1.14 nM, with a B_{max} value of 0.60 (**Figure 3B**).

ImmunoPET imaging and quantitative analysis

To evaluate the clearance of the immunoPET tracer over time, PET scans were performed at multiple time points from 6 h to 120 h p.i. (**Figure 4**). Maximum intensity pro-

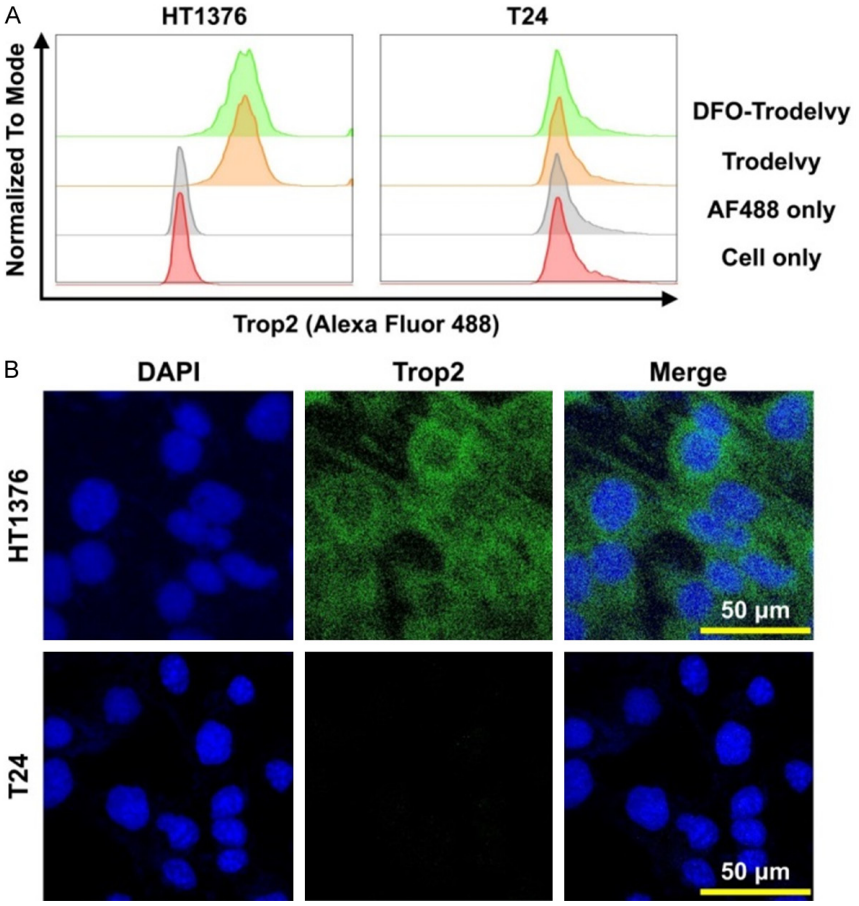

Figure 2. Trop2 expression analysis in HT1376 and T24 bladder cancer cells. A. Flow cytometry analysis of two cell lines treated with 40 μg of Trodelvy and DFO-Trodelvy at 37 °C for 1 h. HT1376 cells exhibited higher Trop2 expression compared to T24 cells. B. Immunofluorescence staining revealed intense Trop2 signals localized to the cell membrane in HT1376 cells, whereas no detectable signals were observed in T24 cells (green for AF488; blue for DAPI). Scale bar: 50 μm.

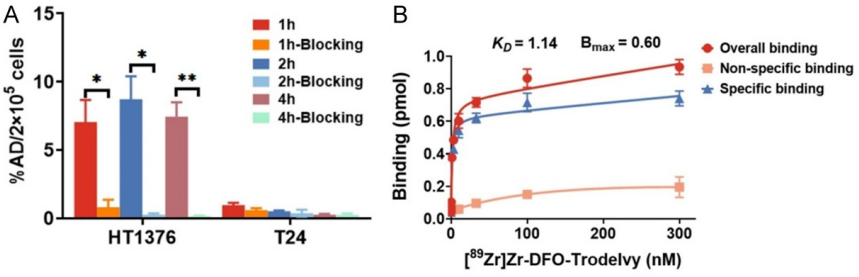

Figure 3. Cell uptake assay and cell binding assay experiment. A. Uptake of the [^{89}Zr]Zr-DFO-Trodelvy in human bladder cancer cell lines. The uptake of HT1376 cells was 7.06 ± 1.32 %AD/2×10^5 at 1 h, 8.72 ± 1.38 %AD/2×10^5 at 2 h, and 7.45 ± 0.86 %AD/2×10^5 at 4 h, reflecting a statistically significant difference compared to the T24 group. The addition of cold, unlabeled Trodelvy demonstrated specificity, leading to a marked reduction in uptake. B. Cell binding affinity of [^{89}Zr]Zr-DFO-Trodelvy with HT1376. The K_D of [^{89}Zr]Zr-DFO-Trodelvy for HT1376 cells was determined to be 1.14 nM, with a B_{max} value of 0.60.

jection (MIP) images demonstrated that [^{89}Zr]Zr-DFO-Trodelvy effectively delineated tumor morphology in HT1376 models as early as 6 h p.i., with tumor uptake progressively increasing and peaking at 48 h, followed by a gradual decline. In contrast, minimal tumor uptake was observed in the blocking and negative control groups.

Quantitative ROI analysis further confirmed these findings, showing sustained and significantly higher tumor uptake in HT1376 tumors (16.33 ± 0.90 %ID/g at 48 h) compared to T24 tumors (6.20 ± 0.99 %ID/g at 48 h, P = 0.0005). Co-injection of 2 mg of unlabeled Trodelvy effectively blocked uptake in HT1376 tumors (4.50 ± 0.51 %ID/g at 48 h, P = 0.0004). No significant differences in tracer uptake was observed among cell groups in the heart (blood), muscle, liver, spleen, or kidney, all of which demonstrated uptake gradually decreasing over time.

A high target-to-non-target ratio was observed at 48 h, characterized by specific tumor accumulation. Collectively, these results highlight the strong detection capability, high specificity, and prolonged tumor retention of [^{89}Zr]Zr-DFO-Trodelvy in Trop2-positive tumors.

Biodistribution results

At the final imaging time point, biodistribution analysis revealed that tumor uptake of [^{89}Zr]Zr-DFO-Trodelvy in HT1376 tumors (16.36 ± 0.95 %ID/g) was significantly greater than in the T24 tumors (6.12 ± 1.96 %ID/g, P = 0.0078) and the blocking group (4.04 ± 0.61 %ID/g, P = 0.0003) (**Figure 5**).

Immunostaining of Trop2 and CD31 in tumor tissues

Following imaging, tumor sections were stained with Trop2 and CD31 antibodies to confirm Trop2 expression and the growth status of the tumors. Immunofluorescence staining showed that Trop2 was prominently expressed in HT1376 tumors, but was not detected in T24 tumors. Additionally, extensive vascularization, marked by CD31 staining, were observed across the cancer models and indicative of active tumor growth (**Figure 6**).

Radiation dosimetry extrapolation to humans

Dosimetry analysis was conducted using OLINDA/EXM software [24]. Estimated human dosimetry was derived from average %ID/g values obtained from serial PET

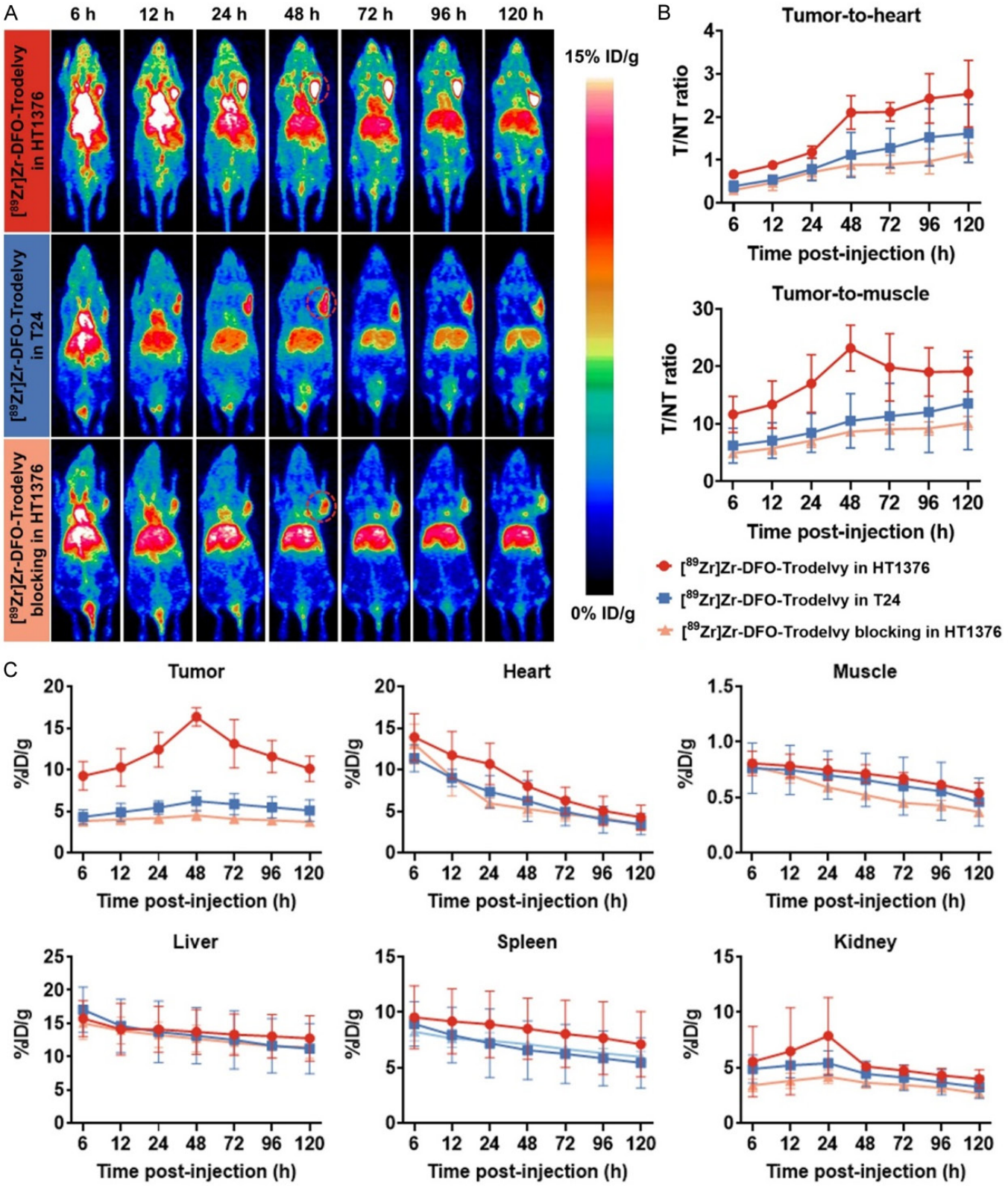

Figure 4. ImmunoPET imaging and *ex vivo* biodistribution of [^{89}Zr]Zr-DFO-Trodelvy in the bladder cancer model. A. ImmunoPET imaging of HT1376 and T24 tumors captured at 6-120 h p.i. B. Tumor-to-heart and tumor-to-muscle ratios obtained from ROI analysis of immunoPET images. C. [^{89}Zr]Zr-DFO-Trodelvy uptake in organs of HT1376 and T24 models, expressed as %ID/g. Data presented as mean ± s.d.

scans on BALB/c mice, converted to %ID in humans. Assuming similar biodistribution in adult humans as in animal models, a monoexponential model was applied to the time-activity curves. OLINDA provides effective dose outputs, and weighting factors from the International Commission on Radiological Protection Publication 103

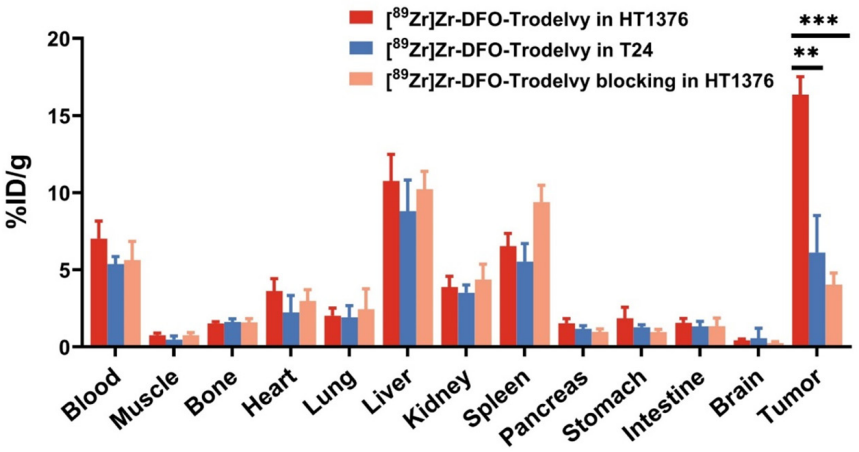

Figure 5. Comparative biodistribution of [^{89}Zr]Zr-DFO-Trodelvy in tumor-bearing mice at 120 h. The biodistribution analysis demonstrates significantly higher uptake of [^{89}Zr]Zr-DFO-Trodelvy in HT1376 tumors compared to T24 tumors and the blocking group, indicating strong tumor-specific accumulation (n = 3). Data presented as mean ± s.d. $^{**}P < 0.01$, $^{***}P < 0.001$.

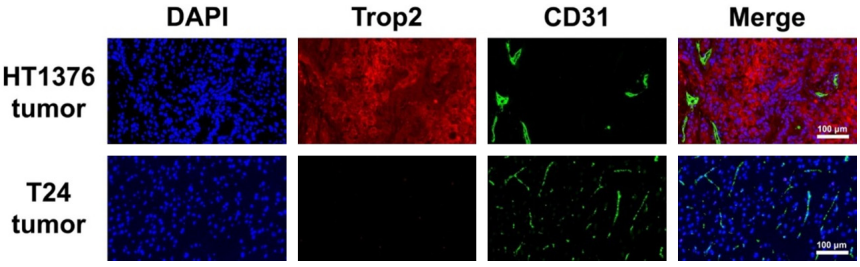

Figure 6. Immunofluorescent analysis in bladder cancer models. Immunofluorescence reveals strong Trop2 staining (red channel) in HT1376 tumors, whereas T24 tumors display only minimal, background-level staining. Scale bar: 100 μm.

were utilized to convert these to absorbed doses for each organ [25]. The radiation dose estimates for human organs, based on biodistribution data, are presented in **Table 1**. The estimated systemic effective dose for an adult woman was 0.492 mSv/MBq, which falls within acceptable limits for conventional nuclear medicine research.

Discussion

Driven by advancements in immunotherapy, the therapeutic approach of utilizing novel molecular markers targeting cancer has gained significant momentum, which in turn is driven by today's advancements in immunotherapy. Trodelvy and its FDA approved use for the treatment of triple-negative breast cancer and refractory urothelial cancer highlights the clinical relevance of Trop2 as a therapeutic agent in oncology. This study further explores the potential of Trodelvy beyond its role as an immunotherapeutic agent through investigating its feasibility for immunoPET imaging to expand its diagnostic and therapeutic use.

In combination with biomarkers, noninvasive immunoPET is a powerful molecular imaging strategy that incorporates high specificity, strong affinity, and superior antibody sensitivity to enable real-time, *in vivo* visualization of Trop2 expression and therapeutic dynamic monitoring [26-29]. In this study, we employed [^{89}Zr]Zr-DFO-Trodelvy for immunoPET imaging in bladder cancer models that was able to achieving high-resolution, quantitative visualization of Trop2 expression *in vivo*.

Our results were in concordance with previous studies, which have reported the feasibility of Trop2-targeted immunoPET for the diagnosis and monitoring of Trop2-positive cancers. Wu et al. [30] developed the ^{89}Zr/^{177}Lu-labeled anti-Trop2 antibody NY003 and evaluated its therapeutic potential through immunoPET and SPECT imaging, as well as radioimmunotherapy (RIT). ImmunoPET and SPECT imaging confirmed the specific accumulation of the radiolabeled antibody in triple-negative breast cancer tumors. The high-dose [^{177}Lu]Lu-DTPA-NY003 group exhibited the strongest antitumor effect, with tumor volumes markedly smaller than those in the control group ($P < 0.05$). This instance of successful integration of diagnostics and therapeutics presents a promising novel strategy for triple-negative breast cancer treatment. Similarly, Li et al. [31] developed the ^{64}Cu/^{177}Lu-labeled anti-Trop2 monoclonal antibody IMB1636 for immunoPET imaging and RIT in a pancreatic cancer model. *In vivo* studies demonstrated that 48 h p.i., the tumor uptake of [^{64}Cu]Cu-NOTA-IMB1636 in the T3M-4 tumor model reached 8.95 ± 1.07 %ID/g, significantly higher than that of the blocking and negative control groups ($P < 0.001$). Furthermore, high-dose [^{177}Lu]Lu-DOTA-IMB1636 exhibited the most potent tumor-suppressive effect, resulting in a standardized tumor volume of 94.24 ± 14.62% at day 14, significantly smaller than that of other control groups ($P = 0.000$-0.047).

In this study, we directly radiolabeled Trodelvy to produce the radiotracer [^{89}Zr]Zr-DFO-Trodelvy, which demonstrated high radiochemical purity and strong in vitro stability. The tracer exhibited robust Trop2-specific targeting in both *in vitro* and *in vivo* settings, enabling noninvasive evaluation of Trop2 expression. Encouraged by these findings, we then performed preclinical evaluations to assess the biodistribution and imaging potential of this ADC radiopharmaceutical in Trop2-targeted PET imaging. [^{89}Zr]Zr-DFO-Trodelvy effectively delineated tumor morphology in HT1376 models as early as 6 h p.i., with tumor uptake progressively increasing and peaking at 48 h (16.33 ± 0.90 %ID/g) before gradually declining. In contrast, signifi-

Table 1. Human organ radiation dosimetry estimation of [^{89}Zr]Zr-DFO-Trodelvy

Target Organ	mSv/MBq
Adrenals	5.32E-03
Brain	1.92E-03
Breasts	5.35E-02
Esophagus	2.01E-02
Eyes	0.00E00
Gallbladder wall	5.47E-03
Left colon	3.20E-02
Small intestine	5.36E-03
Stomach wall	6.72E-02
Right colon	3.19E-02
Rectum	1.57E-02
Heart wall	6.41E-03
Kidneys	4.38E-03
Liver	1.92E-02
Lungs	6.32E-02
Ovaries	2.74E-02
Pancreas	4.47E-03
Salivary glands	4.87E-03
Red marrow	6.27E-02
Osteogenic cells	5.56E-03
Spleen	4.47E-03
Thymus	5.49E-03
Thyroid	2.08E-02
Urinary bladder wall	2.09E-02
Uterus	3.15E-03
Effective dose	4.92E-01

cantly lower tumor uptake was observed in the blocking group (4.50 ± 0.51 %ID/g, P = 0.0004) and the negative control group (6.20 ± 0.99 %ID/g, P = 0.0005).

At 48 h p.i., the tumor-to-muscle and tumor-to-heart ratios indicated that the tracer generated a sufficient PET signal to effectively differentiate tumors from surrounding tissues. These findings suggest that optimal Trop2 immunoPET imaging in clinical settings may require a scanning period exceeding two days, and long-term imaging is recommended to monitor patient prognosis following treatment. The nonspecific tumor uptake observed in the negative control group (T24 models) was likely attributable to the enhanced permeability and retention (EPR) effect, which facilitates the accumulation and prolonged retention of macromolecules within tumors.

This study advances our understanding of Trodelvy's pharmacokinetics and *in vivo* biodistribution, provides human radiation dose estimates, and lays the groundwork for Trop2-targeted therapies. These findings support the future clinical translation of [^{89}Zr]Zr-DFO-Trodelvy immunoPET for bladder cancer.

This present study is subject to several limitations that merit consideration. First, the sample size of animals used in each experiment was relatively small, limiting generalizability and necessitating further studies to confirm reproducibility. Moreover, our future investigations plan to focus on optimizing the molecular size of the ADC by developing smaller F(ab')$_2$ and Fab fragments (~110 kDa and ~55 kDa, respectively), which may retain the high specificity and affinity of Trodelvy while improving pharmacokinetic properties. Furthermore, unlike kit-based radiotracers, ^{89}Zr labeling involves additional steps that could affect the integrity of the antibody. Future research should prioritize the development of novel site-specific labeling strategies to minimize the impact on antibody integrity and enhance clinical applicability.

Conclusion

In summary, we developed [^{89}Zr]Zr-DFO-Trodelvy for immunoPET imaging in bladder cancer models. The tracer demonstrated specific, and sustained tumor accumulation in Trop2-overexpressing models, enabling noninvasive monitoring of Trop2 expression.

Acknowledgements

This work was supported by the University of Wisconsin - Madison and the National Institutes of Health (P30 CA014520), the National Natural Science Foundation of China (82171970, 82472018), Beijing Science Foundation for Distinguished Young Scholars (JQ21025), Beijing Municipal Science & Technology Commission (Z221100007422027), Beijing Nova Program (2024-0484725), National High Level Hospital Clinical Research Funding (Interdisciplinary Research Project of Peking University First Hospital, 2023IR17, 2024IR07; Scientific and Technological Achievements Transformation Incubation Guidance Fund Project of Peking University First Hospital, 2024CX18), the Scientific and technological project in Henan Province (242102311026), Henan Medical Science and Technology Research Program Joint Construction Project (LHGJ20220409), The Henan Association for Science and Technology Youth Talent Support Program (2023HYTP039), The Key Research Project in Henan Universities (23A320059).

Disclosure of conflict of interest

Weibo Cai declares conflict of interest with the following corporations: Portrai, Inc., rTR Technovation Corporation, Four Health Global Pharmaceuticals Inc.

Address correspondence to: Weibo Cai, Departments of Radiology and Medical Physics, University of Wisconsin - Madison, Madison, WI 53705, USA. E-mail: wcai@uwhealth.org; Lei Kang, Department of Nuclear Medicine, Peking University First Hospital, Beijing 100034, China. E-mail: kanglei@bjmu.edu.cn; Liming Li, Department of Radiology, The First Affiliated Hospital of Zhengzhou University, Zhengzhou 450052, Henan, China. E-mail: perfect1989a@163.com

References

[1] Lopez-Beltran A, Cookson MS, Guercio BJ and Cheng L. Advances in diagnosis and treatment of bladder cancer. BMJ 2024; 384: e076743.

[2] Nadal R and Bellmunt J. Management of metastatic bladder cancer. Cancer Treat Rev 2019; 76: 10-21.

[3] Liu J, Gao Y, Song C, Liao W, Meng L, Yang S and Xiong Y. Immunotherapeutic prospects and progress in bladder cancer. J Cell Mol Med 2024; 28: e18101.

[4] Sonpavde G, Pond GR, Rosenberg JE, Bajorin DF, Choueiri TK, Necchi A, Di Lorenzo G and Bellmunt J. Improved 5-factor prognostic classification of patients receiving salvage systemic therapy for advanced urothelial carcinoma. J Urol 2016; 195: 277-82.

[5] Huang W, Zhang Y, Xiao X, Yang Q, Mixdorf JC, Sun X, Engle JW, Fan Y, Li L, Kang L and Cai W. ImmunoPET imaging of Trop2 expression in triple-negative breast cancer using [64Cu]Cu-NOTA-Trodelvy-F(ab')2. Eur J Nucl Med Mol Imaging 2025; [Epub ahead of print].

[6] Huang W, Wang T, Chao F, Yang Q, Mixdorf JC, Li L, Engle JW, Fan Y, Kang L and Cai W. ImmunoPET imaging of Trop2 expression in bladder cancer using [64Cu]Cu-NOTA-Trodelvy. Mol Pharm 2025; 22: 2266-2275.

[7] Liu Y, Huang W, Saladin RJ, Hsu JC, Cai W and Kang L. Trop2-targeted molecular imaging in solid tumors: current advances and future outlook. Mol Pharm 2024; 21: 5909-28.

[8] Pavone G, Motta L, Martorana F, Motta G and Vigneri P. A new kid on the block: sacituzumab govitecan for the treatment of breast cancer and other solid tumors. Molecules 2021; 26: 7294.

[9] Lenárt S, Lenárt P, Šmarda J, Remšík J, Souček K and Beneš P. Trop2: jack of all trades, master of none. Cancers (Basel) 2020; 12: 3328.

[10] Liu X, Ma L, Li J, Sun L, Yang Y, Liu T, Xing D, Yan S and Zhang M. Trop2-targeted therapies in solid tumors: advances and future directions. Theranostics 2024; 14: 3674-92.

[11] Hanna KS, Larson S, Nguyen J, Boudreau J, Bulin J and Rolf M. The role of enfortumab vedotin and sacituzumab govitecan in treatment of advanced bladder cancer. Am J Health Syst Pharm 2022; 79: 629-35.

[12] Abbas M, Heitplatz B, Bernemann C, Boegemann M, Trautmann M, Schrader AJ, Wardelmann E and Schlack K. Immunohistochemical expression of TROP-2 (TACSTD2) on the urothelial carcinoma of the urinary bladder and other types of cancer. Oncol Lett 2023; 26: 527.

[13] De Moura A, Loirat D, Vaillant S, Korbi S, Kiavue N, Bello Roufai D, Escalup L, Desmaris R, Vaflard P, Cottu P, Pierga JY, Bidard FC, Cabel L and Acramel A. Sacituzumab govitecan in metastatic triple-negative breast cancer patients treated at institut curie hospitals: efficacy, safety, and impact of brain metastases. Breast Cancer 2024; 31: 572-580.

[14] Bardia A, Mayer IA, Vahdat LT, Tolaney SM, Isakoff SJ, Diamond JR, O'Shaughnessy J, Moroose RL, Santin AD, Abramson VG, Shah NC, Rugo HS, Goldenberg DM, Sweidan AM, Iannone R, Washkowitz S, Sharkey RM, Wegener WA and Kalinsky K. Sacituzumab govitecan-hziy in refractory metastatic triple-negative breast cancer. N Engl J Med 2019; 380: 741-51.

[15] Huang W, Liang C, Zhang Y, Zhang D, An S, Wu Q, Li J, Zhao H, Wang C, Cui J, Bao Z, Huang G, Wei W and Liu J. ImmunoPET imaging of Trop2 expression in solid tumors with nanobody tracers. Eur J Nucl Med Mol Imaging 2024; 51: 380-94.

[16] Shao F, Pan Z, Long Y, Zhu Z, Wang K, Ji H, Zhu K, Song W, Song Y, Song X, Gai Y, Liu Q, Qin C, Jiang D, Zhu J and Lan X. Nectin-4-targeted immunoSPECT/CT imaging and photothermal therapy of triple-negative breast cancer. J Nanobiotechnology 2022; 20: 243.

[17] Badier L and Quelven I. Zirconium 89 and Copper 64 for ImmunoPET: from antibody bioconjugation and radiolabeling to molecular imaging. Pharmaceutics 2024; 16: 882.

[18] Yoon JK, Park BN, Ryu EK, An YS and Lee SJ. Current perspectives on 89Zr-PET imaging. Int J Mol Sci 2020; 21: 4309.

[19] Huang W, Li L, Zhou Y, Yang Q, Mixdorf JC, Barnhart TE, Hsu JC, Saladin RJ, Liu C, Rosenkrans ZT, Engle JW, Gao J, Kang L and Cai W. Preclinical evaluation of zirconium-89 labeled anti-Trop2 antibody-drug conjugate (Trodelvy) for imaging in gastric cancer and triple-negative breast cancer. Eur J Nucl Med Mol Imaging 2025; 52: 2369-2383.

[20] Kang L, Jiang D, England CG, Barnhart TE, Yu B, Rosenkrans ZT, Yu B, Rosenkrans ZT, Wang R, Engle JW, Xu X, Huang P and Cai W. ImmunoPET imaging of CD38 in murine lymphoma models using 89Zr-labeled daratumumab. Eur J Nucl Med Mol Imaging 2018; 45: 1372-81.

[21] Huang W, Wang T, Qiu Y, Li C, Chen B, Song L, Yang Q, Sun X, Jia B and Kang L. CD38-specific immunoPET imaging for multiple myeloma diagnosis and therapeutic monitoring: preclinical and first-in-human studies. Eur J Nucl Med Mol Imaging 2025; 52: 1791-804.

[22] Chen Z, Yang Q, Song L, Qiu Y, Wang T, Wu S, Huang W, Sun X, Wang A and Kang L. Enhanced theranostic efficacy of 89Zr and 177Lu-labeled aflibercept in renal cancer: a viable option for clinical practice. Mol Pharm 2024; 21: 2544-2554.

[23] Yang Q, Chen Z, Qiu Y, Huang W, Wang T, Song L, Sun X, Li C, Xu X and Kang L. Theranostic role of 89Zr- and 177Lu-labeled aflibercept in breast cancer. Eur J Nucl Med Mol Imaging 2024; 51: 1246-60.

[24] Stabin MG, Sparks RB and Crowe E. OLINDA/EXM: the second-generation personal computer software for internal dose assessment in nuclear medicine. J Nucl Med 2005; 46: 1023-7.

[25] The 2007 recommendations of the international commission on radiological protection. ICRP publication 103. Ann ICRP 2007; 37: 1-332.

[26] Chen H, Zhao L, Pang Y, Shi J, Gao H, Sun Y, Chen J, Fu H, Cai J, Yu L, Zeng R, Sun L, Wu H, Wang Z and Wang F. 68Ga-MY6349 PET/CT imaging to assess Trop2 expression in multiple types of cancer. J Clin Invest 2024; 135: e185408.

[27] Kang L, Li C, Rosenkrans ZT, Engle JW, Wang R, Jiang D, Xu X and Cai W. Noninvasive evaluation of CD20 expression using 64Cu-labeled F(ab')2 fragments of obinutuzumab in lymphoma. J Nucl Med 2021; 62: 372-8.

[28] Huang W, Zhang Y, Cao M, Wu Y, Jiao F, Chu Z, Zhou X, Li L, Xu D, Pan X, Guan Y, Huang G, Liu J, Xie F and Wei W. ImmunoPET imaging of Trop2 in patients with solid tumours. EMBO Mol Med 2024; 16: 1143-61.

[29] Huang W, Cao M, Wu Y, Zhang Y, An S, Pan X, Zhou X, Shao H, Guan Y, Huang G, Gelardi F, Chiti A, Xie F, Liu J and Wei

W. Immuno-PET/CT imaging of Trop2 with [18F]AlF-RESCA-T4 differentiates lung cancer from inflammation. J Nucl Med 2024; 65: 1904-10.

[30] Wu Y, Li T, Zhang X, Jing H, Li F and Huo L. Preclinical evaluation of the theranostic potential of 89Zr/177Lu-labeled anti-TROP-2 antibody in triple-negative breast cancer model. EJNMMI Radiopharm Chem 2024; 9: 5.

[31] Li C, Liu J, Yang X, Yang Q, Huang W, Zhang M, Zhou D, Wang R, Gong J, Miao Q, Kang L and Yang J. Theranostic application of 64Cu/177Lu-labeled anti-Trop2 monoclonal antibody in pancreatic cancer tumor models. Eur J Nucl Med Mol Imaging 2022; 50: 168-83.